Novel Busbar Protection Scheme for Impedance-earthed Distribution Networks

Milan Jankovski, Marjan Popov, Joey Godefrooi, Evita Parabirsing, Ernst Wierenga and Aleksandra Lekić

Abstract—Due to the vast number of substations at the distribution level and increased costs of differential busbar protection, DSOs are in search of cost-effective protection schemes for busbar protection. This includes the use of various communication-based protection schemes, such as the reverse-blocking schemes used at Stedin. However, due to impedance grounding, the single-phase-to-ground short circuit currents have small values in medium voltage impedance-earthed distribution grids. As a result, the reverse-blocking scheme fails to detect this type of fault. This paper introduces a novel distributed protection scheme based on the detection of zero-sequence components of the currents and voltages and the negative-sequence current component. The proposed scheme successfully detects single-phase-to-ground busbar faults by using the standard settings of the widely available overcurrent IEDs, and an IEC 61850 communication between them. Firstly, the detection of the zero- and negative-sequence current components is used to distinguish between a busbar and a feeder fault. Secondly, zero-sequence voltage detection is used to distinguish between the faulty and healthy sections of the busbar when the busbar coupler is opened. This also increases the proposed scheme's reliability by avoiding miss-operation due to human errors during maintenance or testing. The grid is modeled in a Real Time Digital Simulator (RTDS), and a Hardware-in-the-Loop (HiL) simulation is carried out to test the protection scheme. The extensive simulations show the strengths and the limitations of the proposed scheme. Based on the research results, the developed protection scheme is implemented as a standard protection scheme in all of Stedin's new distribution substations.

Keywords—busbar protection, distributed protection scheme, IEC 61850, RTDS testing

I. Introduction

BUSBARS are switchgear components where all the pieces of power system equipment are connected to. They collect the electric power of the incoming feeders and distribute it to the outgoing feeders [1]. As such, they play an important role in the overall reliability of the electrical network. A false trip of the busbar system's protection scheme can threaten the system's stability. It can have a similar effect as a simultaneous fault on all of the elements connected to the

M.Jankovski, M. Popov and A. Lekić are with Delft University of Technology, Delft 2628 CD, The Netherlands (e-mails: milan.jankovski@yahoo.com; M.Popov@tudelft.nl; A.Lekic@tudelft.nl)
J. Godefrooi, E. Parabirsing and E. Wierenga are with Stedin, Rotterdam 3011TA, The Netherlands (e-mails: Joey.Godefrooi@stedin.net; Evita.Parabirsing@stedin.net; Ernst.Wierenga@stedin.net)
Paper submitted to the International Conference on Power Systems Transients (IPST2023) in Thessaloniki, Greece, June 12-15, 2023.

busbar [2]. Nevertheless, at the same time, failing to clear a fault on the busbar or even a slow operation of the protection may lead to cascaded tripping [3]. The busbar differential protection is widely used as a dedicated protection scheme for the busbar systems, which operates on Kirchhoff's current law principle [4]. When applied correctly, it is a fast and a reliable scheme that can fully discriminate between a fault inside the protected zone (the busbar system), and a fault outside the zone [5]. However, when using differential protection from different vendors, the major challenge is the required investment in the IED infrastructure and communication channels among the respective IEDs. That is why power utilities use other alternatives for busbar protection. This is mainly done by the Distribution System Operators (DSOs), which due to their large number of stations and feeders, consider economically more viable alternative solutions [6], [7].

A widely used solution is the reverse-blocking scheme or interlocked overcurrent scheme [8]–[10]. It is a distributed scheme that uses communication between the overcurrent IEDs of the incoming and outgoing feeders connected to the busbar. This scheme is based on the fact that state-of-the-art IEDs can provide an instantaneous start signal, indicating that the IED is measuring an operating value above the set threshold. The incoming feeder overcurrent IED will detect a downstream fault but cannot distinguish between a fault on the busbar or an outgoing feeder, as the fault current level can be similar. That is why the above-mentioned instantaneous start signal from the outgoing feeders IEDs is used to block the operation of the incoming feeders IEDs when the fault is on the outgoing feeder. The IEC 61850 GOOSE communication can be used to exchange these signals over an Ethernet network [11], [12].

Stedin, as a DSO in the Netherlands is responsible for the operation of the sub-transmission and distribution network in the provinces of South Holland, Utrecht, and Zeeland. The reverse-blocking scheme is widely used to protect the busbar systems for lower voltage levels (10 kV, 13 kV, and 21 kV). A standardized 10 kV substation of Stedin is grounded through a zig-zag (ZZ) transformer, a particular type of transformer used to provide a star-point in delta-connected networks, through which the network can be grounded [13], [14]. The resistance through which the ZZ transformer star point is earthed, is chosen in a way to limit the current that passes through the ZZ transformer itself, in a case of a single-phase-to-ground (LG) fault, to 1000 A. This current limitation causes the reverse-blocking scheme's blinding, as the current that passes through the incoming feeder IED is too low to trigger the overcurrent settings [15]. There are some incidents reported

where in these networks, the reverse-blocking scheme was blinded during LG faults and failed to detect them, which led to considerable damage in the network.

This paper addresses the problem of protection blinding and focuses on busbar protection in the case of LG faults in impedance-earthed networks. The method is based on detecting the zero-sequence and negative-sequence current components in the outgoing feeders and the zero-sequence voltage measurements on the busbar. The analysis is conducted using data provided by the substation's IEDs, which use the established Ethernet network in the substation as a means of communication.

The paper is organized as follows. The methodology is explained in Section II, where the concept is thoroughly elaborated. Section III deals with testing the method in a real-time environment using hardware in the loop (HiL) simulation. The applicability of the proposed protection scheme is tested on the typical 10 kV substation design of Stedin, and the results are presented in Section IV. Finally, meaningful conclusions are elaborated in Section V.

II. PROPOSED METHODOLOGY

A typical design of a 10 kV Stedin substation is illustrated in Fig. 1, where the relevant IEDs and circuit breakers (CBs) are also indicated.
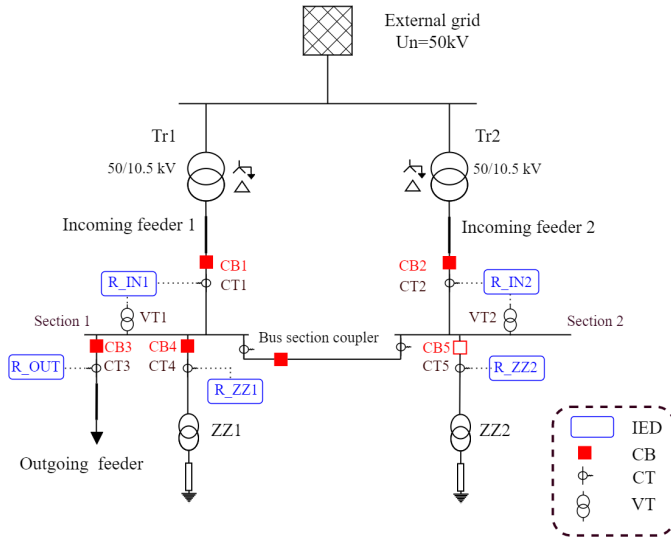

Fig. 1. One-line diagram of a typical 10kV substation of Stedin

The substation is linked to the 50 kV external grid by two identical 50/10.5 kV transformers in a delta-star connection. One ZZ transformer is used to ground the network through a resistance, while the other serves as a backup. The shielding connections of the cable joints in Stedin's 10 kV network are normally 2x6 mm^2 Cu. They can be a bottleneck for the earth-fault current if its magnitude significantly exceeds 1000 A. That is why, according to Stedin's policy, the value of the earth-fault current during LG faults is limited to 1000 A. In order to achieve that, the zero-sequence resistance of the ZZ transformer has to be set to $18\ \Omega$.

The short-circuit power (Sk'') of the external grid, the transformers Tr1 and Tr2 rated power (S_{rated}) and

External grid	Sk$''$ [MVA]	500
Tr1 and Tr2	$S_{rated}[MVA]$	30
	$u_k[\%]$	12.7
Neutral resistor	$R_0[A/sec]$	1000 / 3
Outgoing feeder	R1 [Ω]	0.194
	X1 [Ω]	0.083
	R0 [Ω]	2.46
	X0 [Ω]	0.13

short-circuit voltage (u_k), the outgoing feeder parameters, as well as the value of the neutral resistor are presented in Table I, while the impedances of the incoming feeder, the busbar sections and the winding of the ZZ transformer are neglected because of their small value.

The busbar system consists of two sections (Section 1 and Section 2), which can be coupled or de-coupled through the bus section coupler. For simplicity, the analysis of the LG fault is done for one section only. However, one should keep in mind that the same principles hold for the elements of the second section also. The bus section coupler is open for the following analysis, and the LG fault occurs in Section 1. In this network, there is only one 'source' of a zero-sequence current component, which is the ZZ1 transformer. As transformer Tr1 is with a star-delta connection, according to the theory of symmetrical components [16], it will not provide a zero-sequence current in case of an LG fault in Section 1. This is also noticeable from the zero-sequence representation of the network in case of an LG fault on Section 1 when the bus coupler is open. This representation is shown in Fig. 2, where $X0_{eg}$, $X0_{TR1}$ and $X0_{IN1}$ are the respective zero-sequence impedances of the external grid, transformer Tr1 and the incoming feeder 1. In contrast, $X0_{ZZ\_TR}$ and $R0_{ZZ\_TR}$ are the zero-sequence reactance and resistance of the transformer ZZ1.
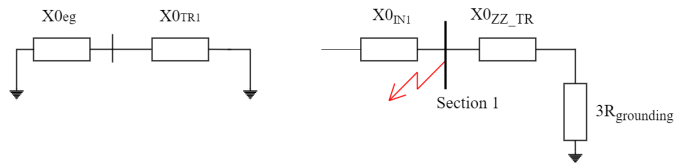

Fig. 2. One-line diagram of the zero-sequence system in case of an LG fault on Section 1

From Fig. 2, it is clear that the zero-sequence component of the fault current circulates only between the ZZ transformer and the fault location. This means that whenever an LG fault occurs on the busbar or the outgoing feeder, the IED R_ZZ1 will detect a sufficient magnitude of a zero-sequence current component. However, when the fault is on the outgoing feeder, the zero-sequence current will also be detected by R_OUT. On the contrary, no significant zero-sequence current will pass through R_OUT when the fault is on the busbar system. Indeed, a small capacitive zero-sequence current will pass due to the cable capacitance [17]. However, the magnitude of this current is small and can be neglected. This unique zero-sequence current distribution gives the basis of the

operation of the proposed scheme.

The earth-fault overcurrent protection setting ($Ie_>$) of R_ZZ1 is used as one of the bases for the proposed scheme. This stage's setting is chosen to be triggered every time an LG fault occurs in the 10 kV busbar system. From [6], the symmetrical components of an LG fault current can be calculated according to equation (1) :

$$I_1 = I_2 = I_0 = \frac{1}{3} * \frac{\sqrt{3}U_n}{Z_1 + Z_2 + Z_0} , \qquad (1)$$

where Z_1, Z_2, and Z_0 are the positive, negative, and zero-sequence impedances seen from the fault location, respectively, and U_n is the nominal voltage of the network. From the data provided in Table I, it can be calculated that in case of an LG fault in the 10kV network, $Z_0 >> Z_1$ and $Z_0 >> Z_2$, and at the same time $Z_0 \approx R0_{ZZ\_TR}$. According to this, the following approximation can be made:

$$Z_1 + Z_2 + Z_0 \approx R0_{ZZ\_TR} \qquad (2)$$

Following this, (1) can be simplified, and I_0 can be calculated as:

$$I_0 = \frac{\sqrt{3}U_n}{3R0_{ZZ\_TR}} \qquad (3)$$

The $Ie_>$ threshold is correspondingly chosen as :

$$Ie_> = 0.75I_0 \qquad (4)$$

The coefficient of 0.75 in (4) accounts for the approximations done in the above-explained equation but also for the imperfections of the IED measurements and any additional small fault resistance.

Equation (3) implies that the zero-sequence current value depends only on the zero-sequence resistance of the ZZ transformer, so it will have an almost identical value regardless of whether the LG fault is on Section 1, the outgoing feeder or on the feeder connecting the ZZ transformer. However, due to selectivity, this protection scheme should not operate for the latter two, and the protection of the respective elements should clear the faults. For this reason, the $Ie_>$ setting of R_ZZ1 has to be blocked from operation in these two cases.

Namely, when the LG fault is on the outgoing feeder, the R_OUT IED will also detect a zero-sequence current component. When this happens, R_OUT sends the instantaneous start signal ($Ie_>.Str$) that blocks the operation of the $Ie_>$ stage of R_ZZ1.

On the other hand, when the fault is on the ZZ transformer feeder, R_ZZ1 will detect the negative-sequence current component, which will be fed in from the external grid. That is why the instantaneous start signal ($Ineg.Str$) of R_ZZ1 is internally used in the same IED to block the $Ie_>$ setting. Both the conditions (zero-sequence and negative-sequence values) start independently. Hence, it is not necessary that one of the conditions should be fulfilled prior to the other one in order to issue the trip command. The interaction between this monitoring of the different values is only when one of the conditions blocks the other. Thus, no time delay is strictly introduced by monitoring different values simultaneously.

From equation (1), we have that in a case of an LG fault, $I_2 = I_0$. Following this and equation (3), we can obtain that the threshold of I_2 can be chosen in the same way as the one of I_e.

If none of the blocking signals is received by R_ZZ1 (i.e., the LG fault is on the busbar), the $Ie_>$ setting is allowed to operate, and after the appropriate time setting expires, it will provide an $Ie_>.Op$ operational signal. However, this operational signal is not coupled as a tripping signal to CB4. Instead, it is sent as an operational signal to both R_IN1 and R_IN2, i.e. it is sent to the IEDs of all of the incoming feeders.

The receiving of the $Ie_>.Op$ is one of the conditions for R_IN1 and R_IN2 to issue the trip signals to CB1 and CB2, respectively. As the busbar protection significantly influences the overall operation and reliability of the network, it was decided to add an additional condition for protection operation. For the second criterion, upon receiving the $Ie_>.Op$ signal from R_ZZ1, the IEDs R_IN1 and R_IN2 will also have to detect a considerable magnitude of zero-sequence voltage, the threshold of which is set to $0.3*Un$, where Un is the nominal voltage of the network. The threshold is chosen in a way that the protection will not operate during normal conditions; however, it is sensitive enough to operate in case of LG faults. This threshold could be a potential jeopardizing factor in case of High-impedance faults (HIF). However, since the Dutch distribution grid is almost 100 % a cable grid, and the developed scheme is a busbar protection scheme, HIFs are not expected.

The zero-sequence voltage detection is not used as the main criterion for the protection scheme as it is a more global parameter for the network; thus, it cannot indicate whether the fault is on the busbar or an outgoing feeder. It is used only to distinguish between the healthy and the faulty section when the bus section coupler is open, and an LG fault occurs on one of the sections.In this topology, since both of the sections are de-coupled, on the healthy section, there will be no zero-sequence voltage detection; thus, that section will continue to operate uninterrupted.

This implies that in the specific case, for R_IN1, both conditions are fulfilled, which makes the IED sends a trip signal to CB1. On the other hand, the healthy section will not experience any zero-sequence voltage, so the respective incoming feeder IED (R_IN2 in this case) will not be able to provide a trip command to the CB (CB2 in the specific case). Additionally, this condition will prevent false trips in case of a human error during maintenance and/or normal operation.

Fig. 3 visually shows the operational logic of the proposed protection scheme.

The same explanation holds when ZZ2 is in service; thus, the same settings and blocking signals are implemented in R_ZZ2 also. The scheme's principle of operation is unchanged when Section 1 and Section 2 are coupled through the bus section coupler. One should note that the value of the thresholds for the zero- and negative-sequence current detection (0.75 * I0), as well as the coefficient for the zero-sequence voltage detection (0.3*Un), should serve only as a guideline, and can be modified based on the network where this protection scheme is to be implemented.
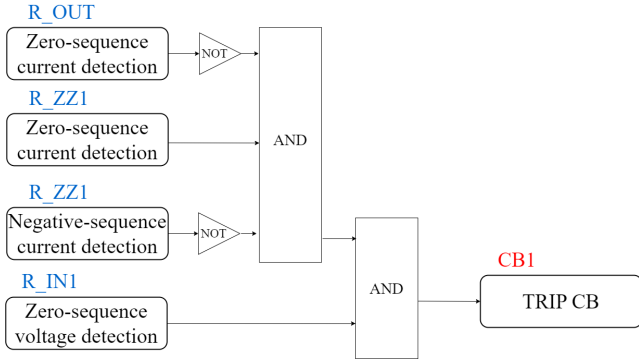
Fig. 3. Operational flowchart of the protection scheme

Stedin, as a stakeholder, decided that no selectivity between the two sections would be introduced when the sections are coupled through the bus section coupler.

A selectivity requirement could be included by adjusting the protection scheme logic. However, more signals will be needed for properly selecting the faulty section by using the CB position signals from both ZZ transformers, the incoming feeders, and the bus section coupler to determine the network topology. Afterward, a separation between the faulty and healthy sections can be achieved based on the network topology and whether the bus section coupler IEDs detect a zero-sequence current. However, this will lead to a more complicated protection solution, which will also be more challenging to test and maintain. This increased complexity could lead to a more error-prone behavior of the protection system, which may result in unwanted trips.

III. METHODOLOGY REAL-TIME IMPLEMENTATION

RTDS®was chosen as a platform to test the proposed methodology, as it is proven to be a reliable platform for modeling and testing protection schemes [18], [19]. The electrical grid under consideration is modeled in the RTDS proprietary software - RSCAD. One physical IED from the manufacturer Sprecher®is connected as a hardware-in-the-loop device. It was intended to have more than one physical relay; however, due to testing limitations, only one relay was managed to be physical. This physical IED represents the IED R_ZZ1, while the rest of the IEDs are virtual. The virtual IEDs are non-directional overcurrent IEDs from the RSCAD proprietary library. Virtual current and voltage transformers from the RSCAD library are used with their default parameters, as presented in Table II and Table III.

TABLE II
CURRENT TRANSFORMER DATA

Ratio	2500/1 A (CT1, CT2)
	600/1 A (CT3, CT4, CT5)
Secondary Side Resistance	0.5 Ω
Secondary Side Inductance	0.0008 H
Burden Series Impedance	0.5 Ω
Burden Series Inductance	0.035 H
Cross-sectional Area	0.0065 m^2
Path Legth	0.5 m

TABLE III
VOLTAGE TRANSFORMER DATA

Ratio	10500/ 110 V
Secondary Side Resistance	11.3 Ω
Secondary Side Inductance	6 H
Secondary Series Resistance	0.00055 Ω
Secondary Series Reactance	0.00029 H
Burden Series Resistance	4.55 Ω
Burden Series Reactance	0.00053 H
Burden Parallel Resistance	2298 Ω
Cross-sectional Area	0.001 m^2
Path Length	1.88 m
Initial Remanence	0.0 p.u.

The simulated currents are fed to the physical IED as analog inputs through an Omicron®CMS-156 amplifier. The tripping and blocking signals between the virtual and physical IEDs are transmitted as GOOSE messages using the IEC 61850 protocol. A necessary modification was done, and the GOOSE messages from the Sprecher IED are not routed through the network switch to the RTDS but are directly coupled. Furthermore, the GOOSE messages from the RTDS are subscribed to an Omicron ISIO box, which translates them to binary outputs and passes them to the Sprecher IED. The overall scheme for the real-time testing of the algorithm can be seen in Fig. 4.
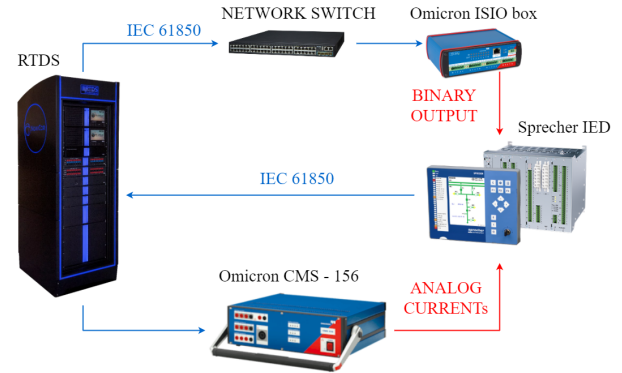

Fig. 4. Hardware-in-the-Loop scheme using an RTDS, Sprecher IED, Omicron amplifier, Omicron ISIO box and a network LAN switch

IV. STUDY CASE

The proposed protection scheme is tested on a typical 10 kV substation design of Stedin. Faults are simulated in five different locations: on both of the sections, on the bus coupler itself, on the outgoing feeder, and the ZZ transformer 1 feeder, as shown in Fig. 5. The simulations are carried out for all of the operational topologies. The provided results are for simulated LG faults involving phase A, with a fault resistance of 0.001 Ω and an inception angle of 0°.

Four different operational topologies can be derived from the basic one-line diagram of the substation:

- Topology 1: The bus section coupler is opened, so both sections are disconnected. Section 1 is energized and
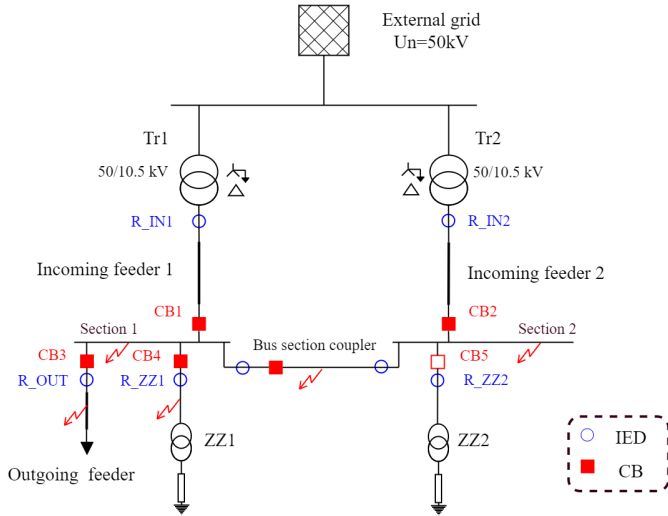
Fig. 5. Test network used for the simulations, with the fault locations

R_ZZ1 and R_ZZ2	Protection setting	I [A]	t [s]
	$Ie_>$	250	0.3
	$Ineg_>$	250	0.3
R_OUT	Protection setting	I [A]	t [s]
	$Ie_>$	150	0.9
R_IN1 and R_IN2	Protection setting	U [%]	t [s]
	U_0	30	0

A. Fault on an outgoing feeder

An LG fault on the outgoing feeder is simulated to show the algorithm's selective operation. The fault is simulated on 50 % of the feeder length. The simulation results for this case, when the grid operates according to Topology 3, are shown in Fig. 6.
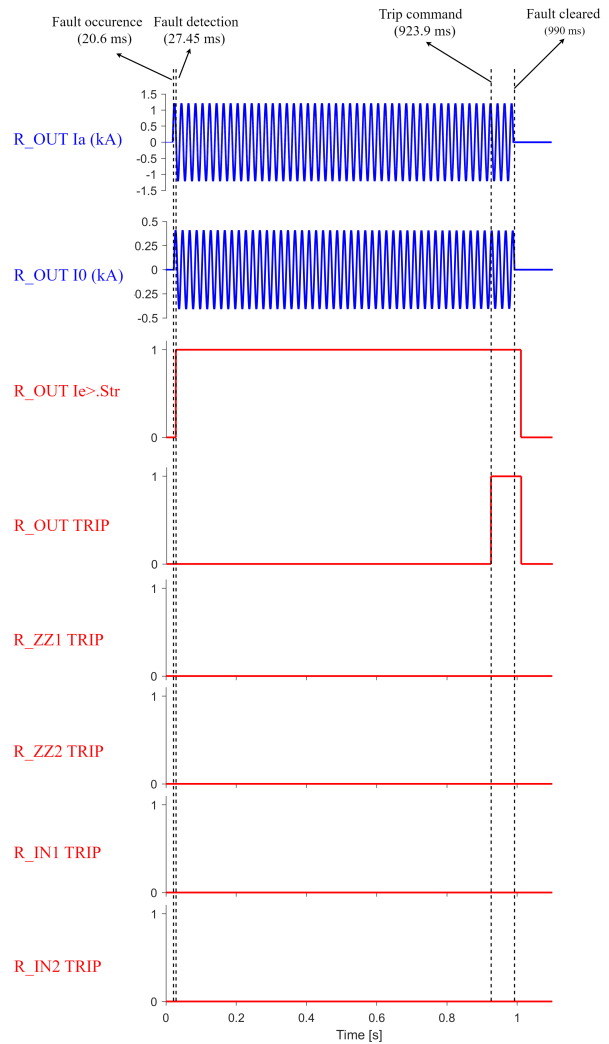

Fig. 6. LG fault on the outgoing feeder (Topology 3)

grounded through Tr1 and ZZ1, respectively, while Tr2 and ZZ 2 are used for the energization and grounding of Section 2.
- Topology 2: The sections are connected through the bus section coupler; however, only Tr1 and ZZ1 are used to energize and ground the busbar system, respectively.
- Topology 3: The sections are connected through the bus section coupler, and both Tr1 and Tr2 are used to energize the busbar system. However, the grounding is done only through ZZ1.
- Topology 4: The sections are connected through the bus section coupler, and both Tr1 and Tr2 are used to energize the busbar system. The grounding is completed by connecting both ZZ1 and ZZ2.

It should be noted that according to Stedin's policy, only one ZZ transformer is allowed to operate at a time, which implies that Topology 4 is not allowed to be an operational one. However, for a short time, when the two sections are to be disconnected, the second ZZ transformer is switched-in before the bus coupler is opened. That is the reason why this topology is also taken as a part of the investigation.

The settings of the IEDs were realised in compliance with the policy of Stedin and with the above-explained calculations, and for this characteristic network they are presented in Table IV. Only the settings that are used in this protection scheme are presented in the table. The time settings for $Ie_>$ of R_ZZ1 and R_ZZ2 are set to 0.3 seconds to comply with the time settings of the already installed busbar protection in Stedin's substations. No time delay is introduced for the zero-sequence voltage detection in R_IN1 and R_IN2, as this is only the second condition for the trip signal from these IEDs. For R_OUT, the time setting of 0.9 seconds is already standardized within Stedin's policy to provide time-selectivity with the descending network. The time setting of $Ineg$ of R_ZZ1 and R_ZZ2 comply with the already established time settings for the protection of the ZZ feeders and they do not have to be time-graded with the rest of the network.

As seen in the figure, the IED R_OUT detects the fault quickly (less than 15 ms) and immediately sends a blocking signal to R_ZZ1. As a result of that, R_ZZ1 is prevented from operating (the $ZZ1\_Ie_>.Op$ signal remains zero during the fault duration). The fault is cleared after around 900 ms (the time setting of the $Ie_>$ stage of R_OUT) by tripping only CB3. In this way, the selectivity of the protection scheme is proved

when a fault occurs on an outgoing feeder. The same results and conclusion are obtained for all four different operational topologies and various places on the feeder where the fault occurs.

B. Fault on the ZZ1 feeder

A particular case that needs to be observed is when the fault occurs on the ZZ transformer 1 feeder, while ZZ1 and ZZ2 are in service. The negative (green) and zero-sequence (purple) current distribution, in this case, is shown in Fig. 7. The dotted purple line represents the capacitive cable current from the outgoing feeder; however, its magnitude is low and does not influence the protection algorithm.
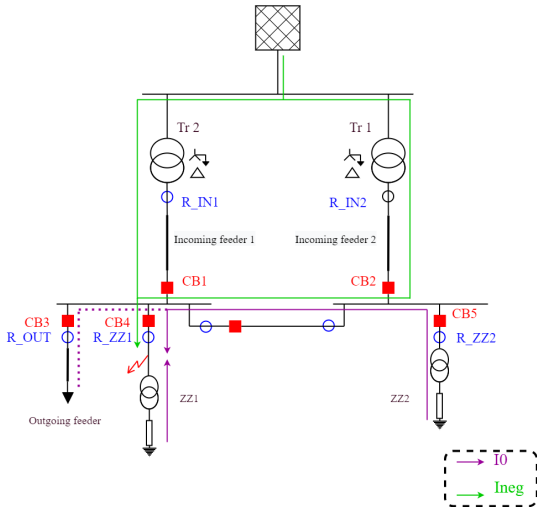

Fig. 7. Zero-sequence and negative-sequence current distribution when two ZZ transformers are connected and an LG fault occurs on one of the ZZ feeders

From the figure, it is evident that both R_ZZ1 and R_ZZ2 will detect zero-sequence current components. However, the negative over-current ($Ineg$) setting of R_ZZ1 is used to block the $Ie_>$ setting in both of them. Following this, the fault is cleared selectively by tripping only CB4. This can be seen in Fig. 8, where the fault occurs on the ZZ transformer 1 feeder while the network operates according to Topology 4. As seen from the results, the Ineg setting of R_ZZ1 operates ($ZZ1\_Ineg_>.Op$) after the respective time setting expires and trips CB 4. At the same time, no operational signal is sent to R_IN1 and R_IN2; thus, no trip signal is sent to CBs 1 and 2 (the signals $BUS1\_TRIP$ and $BUS2\_TRIP$ remain at a value of zero during the fault duration). The same results are observed when the fault occurs on the feeder that connects the second ZZ transformer to the busbar.

C. Busbar section fault

According to the protection scheme logic, when the $Ie_>$ setting of the R_ZZ1 and/or R_ZZ2 is not blocked, the fault is on the busbar system; namely, the fault may occur in Section 1, Section 2, or the bus coupler itself. The distinction between a fault in Section 1 and a fault in Section 2 is made only when the grid operates according to Topology 1, i.e., when the two sections are separated from each other. The results of this simulation are presented in Fig. 9. It can be seen that the
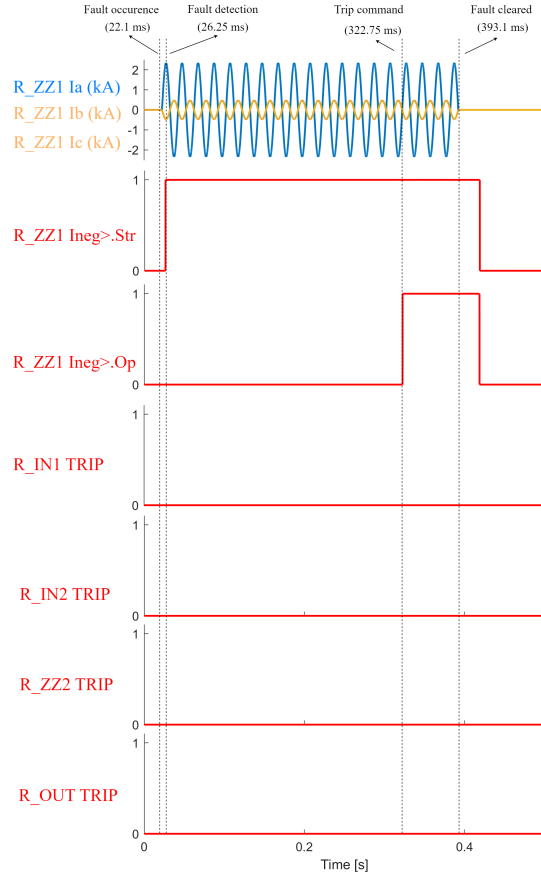

Fig. 8. LG fault on ZZ transformer 1 feeder (Topology 4)

R_ZZ1 detects this fault, and after the appropriate time setting expires, it sends the operating command ($ZZ1\_Ie_>.Op$) to both R_IN1 and R_IN2. However, it is seen that only R_IN1 detects a sufficient magnitude of a zero-sequence voltage, which means that for this IED only, both of the conditions are fulfilled; thus, it sends a trip signal ($BUS1\_TRIP$) to its respective circuit breaker CB1. During this fault, Section 2 continues to operate uninterrupted, which shows the selectivity introduced by adding the second condition. Identical results were observed when the fault occurred in Section 2.

For the other three topologies, when the busbar sections are coupled, faults are simulated on Section 1, Section 2, and the bus section coupler. For all of the topologies, it was observed that the protection scheme successfully detects and clears the fault, regardless of their exact location on the busbar system. This leads to the result that the proposed scheme is able to detect and clear the LG busbar faults. When the two (or multiple) sections of the busbar system are de-coupled, it can selectively clear the fault on the faulty section while the rest remain energized.

D. Angle of inception and fault resistance

Simulations were carried out with different inception angles of the fault: 0°, 30°, 60°, and 90°. For all of the cases, it could be seen that the angle of inception does not influence the protection scheme. The inception angle may add up only to a few more milliseconds of detection time. Since this scheme
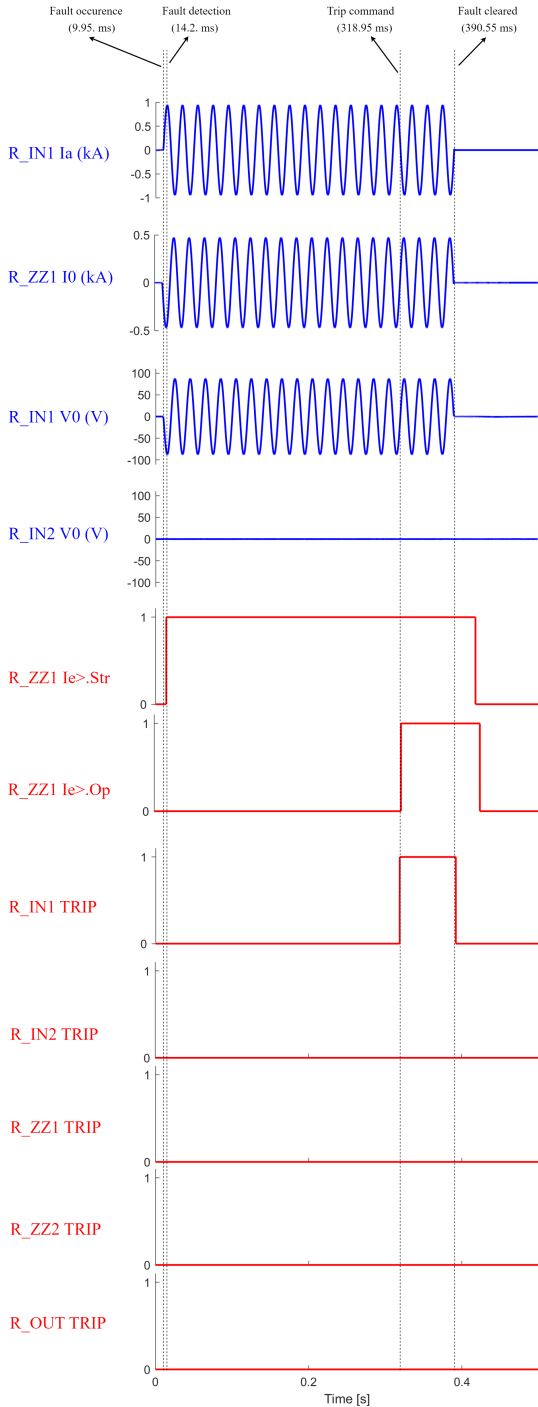
Fig. 9. LG fault on Section 1 (Topology 1)

The goal of this protection scheme is to serve as busbar protection in cable distribution grids, and the fault resistance is not considered as a limitation in the operation of the protection scheme. However, suppose higher fault resistances are to be expected in the network. In that case, the threshold of the zero-sequence voltage setting can be lowered to increase the scheme's sensitivity.

V. CONCLUSIONS

This paper presents a distributed scheme of busbar protection against LG faults in impedance-earthed distribution networks. The protection scheme uses only non-directional over-current IEDs, the most typical protection IEDs in the distribution networks; hence, it is based on the already available infrastructure. Additionally, a zero-sequence voltage detection of the IEDs on the incoming feeders is required, which is also a standard setting in most of the distribution IEDs.

The reason that we developed this scheme is that historically, the 10 kV Stedin grid has been developed in this way, and there are many substations with this topology. Therefore, the proposed solution is innovative, easy, cheap and does not require investment in more relay equipment.

The scheme considers the distribution of the zero-sequence current component during a single-phase-to-ground fault event. This is obtained by the $Ie_>$ settings of the non-directional over-current IEDs on the feeders. Based on the detection of the zero-sequence current, it is decided whether the fault is on the busbar system or on one of the outgoing feeders.

The incoming feeders IEDs also consider the presence of the zero-sequence voltage to distinguish between the faulty and healthy sections when possible.

This implies that the scheme operates on the two-out-of-two principle. Additionally, by introducing two criteria, the chance of the occurrence of missoperation due to maintenance and human errors is reduced.

The IEDs' communication is achieved using the IEC 61850 protocol over an Ethernet network. The paper shows that by using distributed protection schemes, where communication is vital, protection functions can be realized with the already available IED infrastructure.

The scheme is successfully implemented and tested in a real-life environment using HiL simulation. The simulation results prove the selectivity between a fault on an outgoing feeder and a fault on the busbar system. For all of the simulated scenarios, no false trips were identified.

The proposed method has yet to be tested in the case of unbalanced systems. However, it is not expected that a zero-sequence current due to a possible unbalance would jeopardize the scheme. The unbalance would be detected by at least one outgoing feeder (most likely the outgoing feeder where the most significant unbalanced load is connected). As the outgoing feeders IEDs have the same (or smaller) threshold for the zero-sequence current, they will send a blocking signal to prevent false busbar tripping. Therefore, unbalanced systems are not expected to lead to false trips of the busbar system.

is intended for busbar protection in distribution systems (where usually a bigger time margin for clearing the faults is allowed), it is not expected that a small delay will present a jeopardizing factor.

The fault resistance was also varied to see whether or not it affects the protection scheme, mainly because of the introduction of the second criterion for detecting the zero-sequence voltage. The simulations observed that the scheme could not detect the busbar faults when the fault resistance is 13 Ω or higher.

It is also noticed that the communication between the IEDs does not introduce any significant time latency to the protection scheme operation due to the strict time requirements for the GOOSE communication.

VI. References

[1] S. M. Mohan and S. Chatterjee, "Busbar protection – a review," in *2010 IEEE Region 8 International Conference on Computational Technologies in Electrical and Electronics Engineering (SIBIRCON)*, 2010, pp. 755–759. DOI: 10.1109/SIBIRCON.2010.5555158.

[2] Z. Gajić, H. Faramawy, L. He, K. Koppari, L. Max, and M. Kockott, "Modern design principles for numerical busbar differential protection," in *2019 72nd Conference for Protective Relay Engineers (CPRE)*, 2019, pp. 1–16. DOI: 10.1109/CPRE.2019.8765881.

[3] D. Mourad and E. H. Shehab-Eldin, "Simple and adaptive busbar protection scheme considering CT saturation effect," in *2017 Nineteenth International Middle East Power Systems Conference (MEPCON)*, 2017, pp. 71–77. DOI: 10.1109/MEPCON.2017.8301165.

[4] E. J. H. Juan M. Gers, *Protection of electricity distribution networks*. The Institution of Electrical Engineers, London, United Kingdom, 1999.

[5] R. Hughes and E. Legrand, "Numerical busbar protection benefits of numerical technology in electrical substation," in *2001 Seventh International Conference on Developments in Power System Protection (IEE)*, 2001, pp. 463–466. DOI: 10.1049/cp:20010199.

[6] Alstom Grid, *Network Protection & Automation Guide*. Alstom Grid, 2011.

[7] G. Ziegler, *Numerical differential protection*. Publicis Publishing, Erlangen, 2012.

[8] K. Brewis, K. Hearfield, and K. Chapman, "Theory and practical performance of interlocked overcurrent busbar zone protection in distribution substations," in *2001 Seventh International Conference on Developments in Power System Protection (IEE)*, 2001, pp. 475–478. DOI: 10.1049/cp:20010202.

[9] K. M. Tsang and P. Y. Ng, "GOOSE interlock overcurrent protection for 11kv double-busbar substation," in *10th International Conference on Advances in Power System Control, Operation Management (APSCOM 2015)*, 2015, pp. 1–6. DOI: 10.1049/ic.2015.0248.

[10] B. Kasztenny and J. Cardenas, "New phase-segregated digital busbar protection solutions," in *57th Annual Conference for Protective Relay Engineers, 2004*, 2004, pp. 308–338. DOI: 10.1109/CPRE.2004.238553.

[11] J. Das, "Application of Ethernet and IEC 61850 communications," in *Arc Flash Hazard Analysis and Mitigation*. 2021, pp. 533–550. DOI: 10.1002/9781119709787.ch16.

[12] A. Kamaludin, H. Prasetia, and Y. Nugroho, "Implementation of GOOSE for overcurrent relays with non-cascade scheme in medium voltage switchgear as breaker failure and busbar protection system," in *2020 International Conference on Technology and Policy in Energy and Electric Power (ICT-PEP)*, 2020, pp. 179–182. DOI: 10.1109/ICT-PEP50916.2020.9249907.

[13] R. Willheim and M. Waters, *Neutral Grounding in High-voltage Transmission*. Elsevier Publishing Company, 1956. [Online]. Available: https://books.google.nl/books?id=kO4iAAAAMAAJ.

[14] E. Detjen and K. Shah, "Grounding transformer applications and associated protection schemes," *IEEE Transactions on Industry Applications*, vol. 28, no. 4, pp. 788–796, 1992. DOI: 10.1109/28.148444.

[15] M. Jankovski, "Developing and testing a novel busbar protection scheme for impedance-earthed distribution networks," M.S. thesis, Delft University of Technology, 2021.

[16] C. I. Ciontea, "The use of symmetrical components in electrical protection," in *2019 72nd Conference for Protective Relay Engineers (CPRE)*, 2019, pp. 1–8. DOI: 10.1109/CPRE.2019.8765870.

[17] F. G. Limbong, "Investigation of zero sequence capacitive charging at feeder X and Y on ground fault at feeder Z," in *2018 Conference on Power Engineering and Renewable Energy (ICPERE)*, 2018, pp. 1–4. DOI: 10.1109/ICPERE.2018.8739606.

[18] M. Popov, J. Chavez, N. Veera Kumar, S. Azizi, J. Guardado, J. Rueda, P. Palensky, and V. Terzija, "PMU-voltage drop based fault locator for transmission backup protection," English, *Electric Power Systems Research*, vol. 196, pp. 1–8, 2021, ISSN: 0378-7796. DOI: 10.1016/j.epsr.2021.107188.

[19] R. Bakhshi-Jafarabadi, J. Sadeh, J. J. Chavez, and M. Popov, "Two-level islanding detection method for grid-connected photovoltaic system-based microgrid with small non-detection zone," *IEEE Transactions on Smart Grid*, vol. 12, no. 2, pp. 1063–1072, 2021. DOI: 10.1109/TSG.2020.3035126.